Supporting Information to:

Variable Tl, Pb and Cd concentrations and isotope compositions of enstatite and ordinary chondrites – evidence for volatile element mobilization and decay of extinct ^{205}Pb

Carl Palk[1,#], Rasmus Andreasen[1,$], Mark Rehkämper[1*], Alison Stunt[1], Katharina Kreissig[1], Barry Coles[1], Maria Schönbachler[2], and Caroline Smith[3]

[1] Department of Earth Science & Engineering, Imperial College London, London SW7 2AZ, UK

[2] Institute of Geochemistry and Petrology, ETH Zürich, Clausiusstrasse 25, CH-8092 Zürich, Switzerland

[3] Department of Mineralogy, Natural History Museum, London SW7 5BD, UK

* Corresponding author: markrehk@imperial.ac.uk

Current address: School of Earth Sciences, University of Bristol, Bristol BS8 1RJ, UK

$ Current address: Department of Geoscience, Aarhus University, Høegh-Guldbergs Gade 2, 8000 Aarhus C, Denmark

Section 1 – Analytical techniques

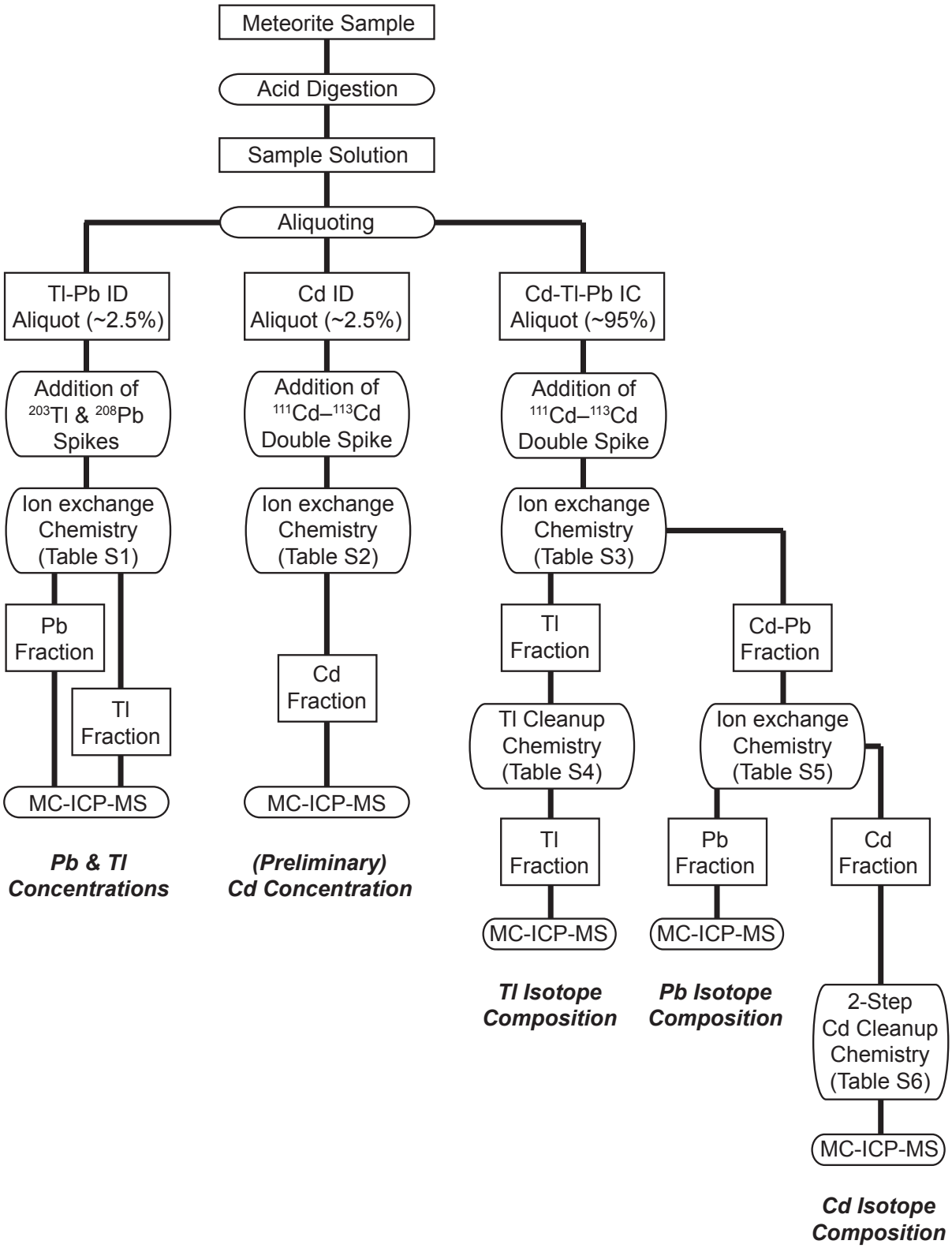


Fig. S1. Flowchart of the full analytical procedure for the determination of Cd-Tl-Pb concentrations and isotope compositions. The final, most precise Cd concentrations are a by-product of the Cd isotope composition measurements with the double spike technique. ID denotes isotope dilution, whilst IC stands for isotope composition.

Table S1. Anion exchange chemistry for the separation of Pb and Tl from sample solution aliquots spiked with ^{203}Tl and ^{208}Pb, for subsequent concentration measurements by isotope dilution MC-ICP-MS (from Baker et al., 2009).

0.2 ml Bio-Rad AG 1-X8 resin, 200-400 mesh	
Teflon PTFE columns with 3 ml reservoirs	
5 ml 0.1 M HCl – 5% SO_2	Resin cleaning
5 ml 0.1 M HCl	Resin cleaning
4 x 0.2 ml 0.2 M HBr – 1% Br_2-H_2O	Resin equilibration
Sample in ~1 ml 0.2 M HBr – 1% Br_2-H_2O	Sample loading
1.4 ml 0.2 M HBr – 0.5M HNO_3 – 1% Br_2-H_2O	Elute matrix
2.2 ml 0.03M HBr – 0.5 M HNO_3 – 1% Br_2-H_2O	Elute & collect Pb
2.2 ml 0.03M HBr – 2 M HNO_3 – 1% Br_2-H_2O	Elute matrix
2.2 ml 0.1 M HCl – 1%Br_2-H_2O	Elute matrix
3.2 ml 0.1 M HCl – 5% SO_2	Elute & collect Tl

Table S2. Anion exchange chemistry for the separation of Cd from spiked sample solution aliquots, for subsequent Cd concentration measurements by isotope dilution MC-ICP-MS (modified from Wombacher et al., 2003).

100 µl Bio-Rad AG 1-X8 resin, 200-400 mesh	
Teflon PTFE columns with 3 ml reservoirs	
750 µl 2M HNO_3	Resin cleaning
100 µl H_2O	Resin cleaning
1300 µl 6 M HCl	Cleaning & conversion to Cl^- form
600 µl 0.5 M HCl	Resin cleaning
300 µl 3 M HCl	Resin equilibration
Sample in ~500 µl 3 M HCl	Sample loading
100 µl 3 M HCl	Elute matrix
1500 µl 0.5 M HCl	Elute matrix (incl. In, Mo)
500 µl 1 M HCl	Elute matrix (incl. Mo)
500 µl 2 M HCl	Elute matrix
600 µl 6 M HCl	Elute matrix (incl. Ag)
600 µl 0.1 M HBr–0.5 M HNO_3	Elute Zn and In
100 µl 2 M HNO_3	Wash
750 µl 2 M HNO_3	Elute & collect Cd

Table S3. Anion exchange chemistry for the separation of a combined Pb-Cd and a Tl fraction from sample solutions for subsequent measurements of isotope compositions.

1 ml Bio-Rad AG 1-X8 resin, 200-400 mesh	
Quartz glass columns with 50 ml reservoirs	
18 ml 2M HNO_3	Resin cleaning
2 ml H_2O	Resin cleaning
18 ml 0.1 M HCl – 5% SO_2	Resin cleaning (Tl elution)
11 ml 0.1 M HCl	Resin cleaning
4 ml 1 M HCl - 2% Br_2-H_2O	Resin equilibration
Sample in 20-25 ml 1 M HCl - 2% Br_2-H_2O	Sample loading
10 ml 0.03 M HBr – 0.5 M HNO_3 - 1% Br_2-H_2O	Elute & collect Pb-Cd
20 ml 0.03 M HBr – 1 M HNO_3 - 1% Br_2-H_2O	Elute & collect Pb-Cd
10 ml 0.01 M HCl – 1% Br_2-H_2O	Elute & collect Pb-Cd
15 ml 0.1 M HCl – 5% SO_2	Elute & collect Tl

Table S4. Anion exchange chemistry for purification of Tl fractions obtained from the 1st-stage chemistry of Table SI-3; following this step Tl is sufficiently pure for subsequent isotopic analysis by MC-ICP-MS (modified from Rehkämper & Halliday, 1999).

100 µl Bio-Rad AG 1-X8 resin, 200-400 mesh	
Teflon PTFE columns with 3 ml reservoirs	
3.1 ml 0.1 M HCl – 5% SO_2	Resin cleaning (Tl elution)
3.1 ml 6 M HCl	Resin cleaning
0.4 ml 6 M HCl – 2% Br_2-H_2O	Resin equilibration
Sample in 0.5 – 1 ml 6 M HCl - 2% Br_2-H_2O	Sample loading
3.1 ml 6 M HCl - 2% Br_2-H_2O	Elute matrix incl. Pb
0.5 ml 12 M HCl - 2% Br_2-H_2O	Elute matrix incl. Pb
3.1 ml 0.01 M HCl - 2% Br_2-H_2O	Elute matrix incl. Pb
1.6 ml 0.1 M HCl – 5% SO_2	Elute & collect Tl

Table S5. Anion exchange chemistry for the separation and purification of Pb and Cd from the combined Pb-Cd fractions obtained from the 1st-stage chemistry of Table SI-3; following this step Pb is sufficiently pure for subsequent isotopic analysis by MC-ICP-MS whilst Cd is further purified (see Table SI-6).

1 ml Bio-Rad AG 1-X8 resin, 200-400 mesh	
Quartz glass columns with 50 ml reservoirs	
10 ml 2 M HNO_3	Resin cleaning
0.5 ml H_2O	Resin cleaning
20 ml 6 M HCl	Cleaning & conversion to Cl^- form
7 ml 0.2 M HBr	Resin equilibration
Sample in 20 – 25 ml 0.2 M HBr	Sample loading
6 ml 0.2 M HBr – 0.5 M HNO_3	Elute matrix
3 ml 0.03 M HBr - 0.5 M HNO_3	Elute matrix
8 ml 0.03 M HBr - 0.5 M HNO_3	Elute and collect Pb
10 ml 0.5 M HCl	Elute matrix
5 ml 2 M HCl	Elute matrix
10 ml 6 M HCl	Elute matrix
1 ml 2 M HNO_3	Wash
10 ml 2 M HNO_3	Elute & collect Cd

Table S6. Chromatographic procedure for purification of Cd from the Cd fractions obtained from the 2nd-stage chemistry of Table SI-5 (modified from Wombacher et al., 2003); following these steps Cd is sufficiently pure for subsequent isotopic analysis by MC-ICP-MS.

Step 1

100 µl Bio-Rad AG 1-X8 resin, 200-400 mesh

Teflon PTFE columns with 3 ml reservoirs

750 µl 2M HNO_3	Resin cleaning
100 µl H_2O	Resin cleaning
1300 µl 6 M HCl	Cleaning & conversion to Cl^- form
600 µl 0.5 M HCl	Resin cleaning
300 µl 3 M HCl	Resin equilibration
Sample in ~500 µl 3 M HCl	Sample loading
100 µl 3 M HCl	Elute matrix
1500 µl 0.5 M HCl	Elute matrix (incl. In, Mo)
500 µl 1 M HCl	Elute matrix (incl. Mo)
500 µl 2 M HCl	Elute matrix
600 µl 6 M HCl	Elute matrix (incl. Ag)
600 µl 0.1 M HBr–0.5 M HNO_3	Elute Zn and In
100 µl 2 M HNO_3	Wash
750 µl 2 M HNO_3	Elute & collect Cd

Step 2

100 µl Eichrom TRU, 100–150 µm

Teflon PTFE columns with 3 ml reservoirs

10 ml 6 M HCl	Resin cleaning
Sample in ~200 µl 8 M HCl	Sample loading; elute & collect Cd (Mo, Sn retained)
200 µl 8 M HCl	Elute & collect Cd (Mo, Sn retained)
1400 µl 6 M HCl	Elute & collect Cd (Mo, Sn retained)

Section 2 – Terrestrial Pb contamination of meteorites

Text – Modeling to estimate terrestrial Pb contamination of meteorites

Previously, Nielsen et al. (2006) and Baker et al. (2010) carried out mass balance calculations to estimate the extent of anthropogenic Pb contamination for iron meteorites and carbonaceous chondrites, respectively. These calculations employ an estimate for the present-day isotope composition of the indigenous meteoritic (or non-contaminated) Pb component. For iron meteorites and carbonaceous chondrites, such estimates are relatively straightforward, as the low U/Pb and Th/Pb ratios of the samples severely restrict radiogenic ingrowth of Pb over time.

The presence of radiogenic Pb in enstatite chondrites (ECs) and ordinary chondrites (OCs) requires a more sophisticated approach to estimate the present-day composition of the meteoritic (non-contaminated) Pb component present in a meteorites sample. In detail, ingrowth of radiogenic Pb by in situ decay of ^{232}Th, ^{235}U and ^{238}U must be considered. As the U and Th concentrations of the samples were not determined in this study but are required for the calculations, we applied literature abundance data (where available) or assumptive estimates. The calculations employ further straightforward assumptions, and the final results are hence model-based estimates of the molar fractions indigenous meteoritic Pb ($f_{met\text{-}Pb}$) present in the analyzed samples. Whilst the terrestrial Pb contaminant is likely to be predominantly of anthropogenic origin it may also feature a natural component.

Modeling approach

The modeling assumes that the meteorites initially had the primordial isotope composition given by Canyon Diablo Pb (Tatsumoto et al., 1973), whereby the concentrations of initial primordial Pb (at 4.566 Ga) and present-day meteoritic Pb are treated as linked unknowns. The isotope composition of the meteoritic Pb is altered by radiogenic additions of ^{206}Pb, ^{207}Pb and ^{208}Pb until the present day, based on the assigned U and Th contents. For seven of 8 ECs and nine of 20 OCs, U and Th concentrations determined by mass spectrometry (either ID-TIMS or ICP-MS) were available (Table S7). These data reveal that U and Th show some but only relatively limited variability in different samples of the same meteorite and between different meteorites of the same class or group. In addition, a small systematic offset in U and Th contents is apparent between the ECs and OCs of the sample suite but not between EH and EL chondrites or L and LL chondrites (Table S7). These observations justify the use of literature U, Th concentrations as a basis to obtain realistic estimates for the time-integrated ingrowth of radiogenic Pb in the samples. In addition, it also allows the calculation of meaningful overall mean U and Th abundances of 7.5 ± 1.3 ng/g (1sd) and 29.3 ± 3.0 ng/g (1sd), respectively, for ECs and of 10.7 ± 2.7 ng/g and 35.2 ± 4.9 ng/g for the OCs (Table S7). These mean values were subsequently employed to derive model-dependent estimates for ingrowth of radiogenic Pb in samples for which U, Th data were not available in the literature (Table S8).

The present-day composition of the terrestrial contaminant was estimated based on the approach developed by Göpel et al. (1985) to evaluate Pb contamination of iron meteorites. The same methods were previously employed by Nielsen et al. (2006) and Baker et al. (2010). In detail, the Pb isotope ratios of the contaminant were assumed to correlate in 3-isotope plots, with arrays defined by the following equations:

$^{207}Pb/^{204}Pb = 0.0898 \times {}^{206}Pb/^{204}Pb + 13.92\ (\pm 0.3)$ (Eq. 1)

$^{208}Pb/^{204}Pb = 0.0697 \times {}^{206}Pb/^{204}Pb + 25.3\ (\pm 0.5)$ (Eq. 2)

The modeling thereby evaluated an intermediate Pb isotope composition of $^{206}Pb/^{204}Pb = 18.0$ and two extreme cases with contaminant $^{206}Pb/^{204}Pb$ ratios of 16.5 and 19.5.

The estimates for the indigenous meteoritic Pb present in the analyzed samples were then obtained with the aid of the spreadsheet-based solver available in Microsoft Excel for Mac 2011 (v 14.7.3). The numerical solver was employed to minimize the (relative) differences in the $^{206}Pb/^{204}Pb$, $^{207}Pb/^{204}Pb$ and $^{208}Pb/^{204}Pb$ ratios that were estimated as described above and obtained by measurement (Tables 1, S8). The former were thereby calculated by mixing meteoritic Pb (= indigenous primordial Pb + in situ produced radiogenic Pb) with variable proportions of terrestrial contaminant Pb (with a variable composition; see Eqs. 1, 2). The isotopic offset between the results obtained in the mixing calculations and the data was reduced by varying the initial concentration of primordial Pb in the meteorites (at 4.566 Ga). The measured total Pb contents of the samples (= meteoritic Pb + contaminant Pb; Table S8) thereby act as an additional constraint for the modeling, which provides the present-day molar fraction of meteoritic Pb in the meteorite samples as a final result ($f_{met\text{-}Pb}$; Table S8; also shown in Table 1 of the main text).

Given that the U and Th concentrations of the samples were not measured but are either based on literature results for the same meteorites or assumed to be equivalent the mean U, Th contents of ECs or OCs (Table S7), the modeling makes explicit allowances for the uncertainty of the abundance data. In detail, the ranges of $f_{met\text{-}Pb}$ values summarized in Table S8 (and Table 1) are a consequence of varying the U and Th concentrations based on the uncertainties obtained for the EC and OC mean values (Table S7). The calculations thereby applied uncertainties for U and Th concentrations of ±25% and ±15%, respectively, for the ECs and of ±35% and ±20% for the OCs. These uncertainties likely provide a conservative estimate for the variability of U and Th within different samples of the same meteorite but may well underestimate the uncertainty associated with using mean U, Th concentrations of ECs/OCs to characterize various distinct meteorites of the same class (Table S7). Consequently, the model-based estimates of $f_{met\text{-}Pb}$ for meteorites with no published U, Th data must be considered with care and these results are hence given in parentheses, both in Table S8 and Table 1 of the main text.

The solutions obtained for $f_{met\text{-}Pb}$ by iteration were deemed reasonable when residual differences between the measured Pb isotope data and calculated results were ≤1.0 for $^{206}Pb/^{204}Pb$, $^{207}Pb/^{204}Pb$ and ≤1.5 for $^{208}Pb/^{204}Pb$. For the great majority of samples, the modeling yielded optimized Pb isotope compositions that were associated with residuals much smaller than 0.1 for all three ratios. However, for a few meteorites, and particularly those with radiogenic Pb ($^{206}Pb/^{204}Pb$ >25), the residual differences were larger, generally for either $^{206}Pb/^{204}Pb$ *and* $^{207}Pb/^{204}Pb$ or for $^{208}Pb/^{204}Pb$. This most likely reflects the presence of U- or Th-rich phases in the samples, whereby the latter are then characterized by Th/U ratios that deviate significantly from the 'normal' range of values that was assumed in the modeling (Table S7). In such cases, the solver optimization was modified to minimize only the residuals for $^{206}Pb/^{204}Pb$ and $^{207}Pb/^{204}Pb$; these samples are marked (by an *) in Table S8.

Modeling results

The $f_{met\text{-}Pb}$ data of Table S8 reveal that the extent of Pb contamination is highly variable for the meteorite samples, ranging from nearly 0% to 100%. The calculated extent of contamination is

thereby in good agreement with qualitative assessments based on the highly variable $^{204}Pb/^{203}Tl$ ratios (e.g., Fig. 2b). In the following, the results are examined in more detail to assess how robust and meaningful the modeled $f_{met\text{-}Pb}$ data are.

With the exception of Tuxtuac, all calculations for meteorites with Pb isotope compositions that fall in between values for primordial Pb ($^{206}Pb/^{204}Pb$ = 9.307) and terrestrial contaminant Pb ($^{206}Pb/^{204}Pb$ = 16.5 to 19.5) yield $f_{met\text{-}Pb}$ estimates that vary by less than ±15% (in absolute terms) about the median value (Table S8). For most meteorites with Pb isotope ratios in the range of contaminant Pb, with $^{206}Pb/^{204}Pb$ between about 17 and 20, only maximum $f_{met\text{-}Pb}$ estimates (e.g., $f_{met\text{-}Pb} < 0.07$) are given, because results of $f_{met\text{-}Pb} \leq 0.04$ were assumed to be identical to $f_{met\text{-}Pb} = 0$, given the inherent uncertainties of the model-based calculations. Considering the relatively small ranges of $f_{met\text{-}Pb}$ values that were obtained in the calculations, despite taking into account reasonably large uncertainties for the Pb isotope composition of the contaminant and the U, Th concentrations of the meteorites, the results obtained for samples with unradiogenic Pb with $^{206}Pb/^{204}Pb < 20$ are likely to be fairly robust. The calculations are thereby most reliable for meteorites (i) where U, Th concentrations are available in the literature and (ii) with relatively unradiogenic Pb isotope ratios of $^{206}Pb/^{204}Pb < 16$ where $f_{met\text{-}Pb}$ estimates generally vary by less than ±10% about the median value (Table S8).

The model calculation to estimate $f_{met\text{-}Pb}$ are less robust for samples with radiogenic Pb isotope compositions of $^{206}Pb/^{204}Pb > 25$. This is related to the modeling approach, which applies estimated rather than measured U and Th abundances to quantify the in situ ingrowth of radiogenic Pb in the samples and the $f_{met\text{-}Pb}$ estimates determined for such meteorites should hence be viewed with caution. This conclusion is underlined by the observation that the iteration for most samples with $^{206}Pb/^{204}Pb > 25$ did not yield sufficiently low residuals when all three Pb isotope ratios were optimized simultaneously, most likely because the meteorites were characterized by distinctly non-average Th/U ratios. Furthermore, highly variable $f_{met\text{-}Pb}$ estimates were returned for most of these samples, for example with Saratov showing $f_{met\text{-}Pb}$ = 38% – 91%.

Application of $f_{met\text{-}Pb}$ to determine $^{204}Pb/^{203}Tl$ ratios that are corrected for terrestrial Pb contamination

Given the evidence for essentially ubiquitous addition of terrestrial Pb to the meteorites, it is useful to carry out ^{205}Pb-^{205}Tl isochron calculations with $^{204}Pb/^{203}Tl$ data that are corrected for this contamination, as shown in Fig. 5. The present-day indigenous meteoritic $^{204}Pb/^{203}Tl$ of relevant samples (Table 3) were thereby calculated by correcting the measured $^{204}Pb/^{203}Tl$ ratios (Table 1) for the presence of terrestrial Pb, using the $f_{met\text{-}Pb}$ values (Tables 1, 3) that were determined as described above. The quoted uncertainties shown for the corrected $^{204}Pb/^{203}Tl$ data (Table 3) were determined by propagating the measurement errors for $^{204}Pb/^{203}Tl$ (Table 1) and the uncertainty of the $f_{met\text{-}Pb}$ values (Tables 1, 3).

Table S7. Published U-Th concentration data determined by mass spectrometry for samples relevant to this study

	U ng/g	Th ng/g	Th/U	Reference
EH Chondrites				
Abee	7			Kaltenbach 2013
	8.0	29.0	3.63	Barrat et al. 2014
Mean	7.5	29.0	3.63	
Indarch	8.33			Manhes & Allegre 1978
	9.44	27.37	2.90	Dauphas & Pourmand 2011
	8			Kaltenbach 2013
	6.0	29.0	4.83	Barrat et al. 2014
	8.5	27.5	3.24	Barrat et al. 2014
	7.7	29.0	3.77	Barrat et al. 2014; U value in () in paper
Mean	8.0	28.2	3.68	
St. Marks	8.13			Manhes & Allegre 78
	8.39	27.60	3.29	Dauphas & Pourmand 2011
	8.9	29.2	3.28	Barrat et al. 2014
Mean	8.5	28.4	3.29	
EL Chondrites				
MAC 02839	8.8	34.4	3.91	Barrat et al. 2014; data for MAC02837 which is paired
PCA 91020	7.7	33.6	4.36	Barrat et al. 2014
Atlanta	4.37	25.7	5.88	Shinotsuka et al. 1995
Daniel's Kuil	8.14	29.34	3.60	Dauphas & Pourmand 2011
Khairpur	6.84	25.77	3.77	Dauphas & Pourmand 2011
Mean ECs	**7.5**	**29.3**	**4.0**	
1sd	**1.3**	**3.0**	**0.8**	
RSD (%)	**17**	**10**	**19**	
L Chondrites				
Saratov	20			Kaltenbach 2013
	19			Kaltenbach 2013
	10			Kaltenbach 2013
	15	37.5	2.50	Andersen et al. 2015; Th calculated from published Th/U
Mean	16	37.5	2.50	
Tennasilm	11.27	39.1	3.47	Unruh 1982
	11.20	39.2	3.50	Unruh 1982
	11.77	40.8	3.47	Unruh 1982
Mean	11.41	39.7	3.48	
Ausson	6.0	24.0	4.00	Göpel et al. 1994; Th calculated from published Th/U ratio
Barwell	7.6	26.6	3.50	Göpel et al. 1994; Th calculated from published Th/U ratio
	7.9	30.8	3.90	Göpel et al. 1994; Th calculated from published Th/U ratio
	9.24	36.7	3.97	Göpel et al. 1994; Th calculated from published Th/U ratio
	9.35	38.9	4.16	Unruh 1982
	9.84			Unruh 1982
Mean	8.8	33.3	3.88	
Marion (Iowa)	10.0	34.0	3.40	Göpel et al. 1994; Th calculated from published Th/U ratio
	9.9	35.6	3.60	Göpel et al. 1994; Th calculated from published Th/U ratio
	6.35	27.4	4.31	Hagee et al. 1990
	10.40	35.5	3.41	Hagee et al. 1990
Mean	9.2	33.1	3.68	
LL Chondrites				
Soko-Banja	12.42	39.01	3.14	Dauphas & Pourmand 2011
Olivenza	10.90	39.7	3.64	Hagee et al. 1990
Tuxtuac	4.6	20.2	4.40	Göpel et al. 1994; Th calculated from published Th/U ratio
	18.01	50.0	2.78	Dauphas & Pourmand 2011
Mean	11.3	35.1	3.59	
Mean OCs	**10.7**	**35.2**	**3.49**	
1sd	**2.7**	**4.9**	**0.4**	
RSD (%)	**25**	**14**	**13**	

The mean U, Th concentrations and Th/U ratios of enstatite and ordinary chondrites were calcualted using the quoted means of individual meteorites, when several results were available.

Table S8. Estimated mass fractions of meteoritic Pb in the samples (f_{met-Pb}) and key paramters that constrain the estimates

	U ng/g (a)	Th ng/g (a)	Pb ng/g (b)	$^{206}Pb/^{204}Pb$ (b)	$^{207}Pb/^{204}Pb$ (b)	$^{208}Pb/^{204}Pb$ (b)	f_{met-Pb} (c)
EH Chondrites							
Abee	7.5	29.0	2497	10.336	10.972	30.481	0.83 - 0.87
Indarch	8.0	28.2	31538	18.137	15.143	38.076	≤0.10
St. Marks	8.5	28.4	205	16.625	14.794	36.424	0.27 - 0.53
EL Chondrites							
MAC 02839	8.8	34.4	1653	9.584	10.48	29.765	≥0.98
PCA 91020	7.7	33.6	1234	9.609	10.496	29.842	≥0.98
Atlanta	4.37	25.7	469	17.868	15.32	38.028	≤0.19
Daniel's Kuil	8.14	29.34	7978				
Khairpur	6.84	25.77	251	10.976	11.339	31.364	0.88 - 0.99
NWA 3134	(8.0)	(30.9)	47	28.085	21.977	52.917	(0.32 - 0.89)*
L Chondrites							
Mezö-Madaras	(10.7)	(35.2)	617	11.292	11.518	31.313	(0.76 - 0.88)
Saratov	16	37.5	81	25.53	20.426	44.199	0.38 - 0.91*
Tennasilm	11.41	39.7	484	14.616	13.555	34.643	0.35 - 0.58
Ausson	6.0	24.0	4850	18.415	15.703	38.456	≤0.07
Alfianello	(10.7)	(35.2)	1645	17.15	15.72	36.97	(0.05 - 0.33)
New Concord	(10.7)	(35.2)	597	19.6	16.42	39.67	(≤0.14)
Mocs 54773	(10.7)	(35.2)	59	41.616	30.012	58.962	(0.68 - 0.74)*
Mocs 54647	(10.7)	(35.2)	55	39.19	28.432	59.271	(0.43 - 0.92)*
Barwell	8.8	33.3	100	26.449	21.223	45.83	0.20 - 0.40*
Marion (Iowa)	9.2	33.1	21598	18.379	15.64	38.405	≤0.07
LL Chondrites							
Bishunpur	(10.7)	(35.2)	1239	15.435	13.996	35.458	(0.18 - 0.37)
Parnallee	(10.7)	(35.2)	265	11.85	11.93	31.95	≥0.82
Benares	(10.7)	(35.2)	1899	18.21	15.76	38.77	(≤0.11)
Soko-Banja	12.42	39.01	564	13.057	12.608	33.108	0.53 - 0.72
Khanpur	(10.7)	(35.2)	656	18.752	16.375	38.223	(≤0.17)
Olivenza	10.90	39.7	486	13.17	12.62	33.18	0.53 - 0.71
Tuxtuac	11.3	35.1	267	18.089	15.465	38.870	0.10 - 0.46*
Appley Bridge	(10.7)	(35.2)	714	17.37	15.25	37.210	(≤0.27)
Dhurmsala	(10.7)	(35.2)	694	19.411	16.344	39.317	(≤0.13)
Mangwendi	(10.7)	(35.2)	503	15.87	14.58	35.800	(0.19 - 0.43)

(a) Values without () are from the literature; see Table S7 for sources. Calculations for samples without published U, Th data are based on the mean U and Th concentrations determined for ECs and OCs in Table S7, as shown in ().

(b) Pb concentration and isotope data are from this study.

(c) The f_{met-Pb} values denote the estimated fraction of meteoritic Pb in the samples, calculated as described in the text, constrained by parameters shown in this table, whereby the stated concentrations of U and Th are assumed to have uncertainties of ±25% and ±15% for the ECs and ±35% and ±20% for the OCs (see Table S7). Given these uncertainties, the estimates are assigned $f_{met-Pb} = 0$ if numerical results are within 4% (absolute) of 0. Solver calculations for samples marked with an * were optimized using $^{206}Pb/^{204}Pb$ and $^{207}Pb/^{204}Pb$ only, most likely because the samples featured unusual Th/U ratios (see text).

References

Andersen M. B., Elliott T., Freymuth H., Sims K. W. W., Niu Y., and Kelley K. A. (2015) The terrestrial uranium isotope cycle. *Nature* **517**, 356-359.

Baker R. G. A., Rehkämper M., Hinkley T. K., Nielsen S. G., and Toutain J. P. (2009) Investigation of thallium fluxes from subaerial volcanism—Implications for the present and past mass balance of thallium in the oceans. *Geochim. Cosmochim. Acta* **73**, 6340-6359.

Baker R. G. A., Schönbächler M., Rehkämper M., Williams H., and Halliday A. N. (2010) The thallium isotope composition of carbonaceous chondrites – new evidence for live ^{205}Pb in the early solar system. *Earth Planet. Sci. Lett.* **291**, 39-47.

Barrat J. A., Zanda B., Moynier F., Bollinger C., Liorzou C., and Bayon G. (2012) Geochemistry of CI chondrites: major and trace elements, and Cu and Zn isotopes. *Geochim. Cosmochim. Acta* **83**, 79-92.

Dauphas N. and Pourmand A. (2011) Hf–W–Th evidence for rapid growth of Mars and its status as a planetary embryo. *Nature* **473**, 489-492.

Göpel C., Manhès G., and Allègre C. J. (1985) U-Pb systematics in iron meteorites: Uniformity of primordial lead. *Geochim. Cosmochim. Acta* **49**, 1681-1695.

Göpel C., Manhès G., and Allègre C. J. (1994) U-Pb systematics of phosphates from equilibrated ordinary chondrites. *Earth Planet. Sci. Lett.* **121**, 153-171.

Hagee B., Bernatowicz T. J., Podosek F. A., Johnson M. L., Burnett D. S., and Tatsumoto M. (1990) Actinide abundances in ordinary chondrites. *Geochim. Cosmochim. Acta* **54**, 2847-2858.

Kaltenbach A. (2012) Uranium isotopic analysis of terrestrial and extraterrestrial samples. PhD thesis. University of Otago, Dunedin, New Zealand.

Manhes G. and Allègre C. J. (1978) Time differences as determined from the ratio of lead 207 to lead 206 in concordant meteorites. *Meteoritics* **13**, 543-548.

Nielsen S. G., Rehkämper M., and Halliday A. N. (2006) Thallium isotopic variations in iron meteorites and evidence for live lead-205 in the early solar system. *Geochim. Cosmochim. Acta* **70**, 2643-2657.

Rehkämper M. and Halliday A. N. (1999) The precise measurement of Tl isotopic compositions by MC-ICPMS: Application to the analysis of geological materials and meteorites. *Geochim. Cosmochim. Acta* **63**, 935-944.

Shinotsuka K., Hidaka H., and Ebihara M. (1995) Detailed abundances of rare earth elements, thorium and uranium in chondritic meteorites: An ICP-MS study. *Meteoritics* **30**, 694-699.

Tatsumoto M., Knight R. J., and Allègre C. J. (1973) Time differences in the formation of meteorites as detemined from the ratio of lead-207 to lead-206. *Science* **180**, 1278-1283.

Unruh D. M. (1982) The U-Th-Pb age of equilibrated L chondrites and a solution to the excess radiogenic Pb problem in chondrites. *Earth Planet. Sci. Lett.* **58**, 75-94.

Wombacher F., Rehkämper M., Mezger K., and Münker C. (2003) Stable isotope compositions of cadmium in geological materials and meteorites determined by multiple collector-ICPMS. *Geochim. Cosmochim. Acta* **67**, 4639-4654.